Pis'ma v ZhETF, vol. 80, iss. 10, pp. 721 – 726 © 2004 November 25

Radiative parton energy loss and jet quenching in high-energy heavy-ion collisions[1)]

B. G. Zakharov

Fakultät für Physik, Universität Bielefeld, D-33501 Bielefeld, Germany

L.D. Landau Institute for Theoretical Physics RAS, 117334 Moscow, Russia

Submitted 25 October 2004

We study within the light-cone path integral approach [3] the effect of the induced gluon radiation on high-p_T hadrons in high-energy heavy-ion collisions. The induced gluon spectrum is represented in a new form which is convenient for numerical simulations. For the first time computations are performed with a realistic parametrization of the dipole cross section. The results are in reasonable agreement with suppression of high-p_T hadrons in Au+Au collisions at $\sqrt{s} = 200$ GeV observed at RHIC.

PACS: 12.38.−t

1. One of the most interesting results obtained at RHIC is the suppression of high-p_T hadrons in Au+Au collisions (for a review of the data, see [1]). It is widely believed that parton energy loss due to the induced gluon radiation caused by multiple scattering in the quark-gluon plasma (QGP) produced in the initial stage of nucleus-nucleus collisions plays a major role in this phenomenon (usually called the jet quenching) [2 – 7] (for a review, see [8]). The most general approach to the induced gluon emission is the light-cone path integral (LCPI) approach developed in [3] (see also [9, 10, 8]). It treats accurately the mass and finite-size effects, and applies at arbitrary strength of the Landau–Pomeranchuk–Migdal (LPM) effect [11, 12]. Other available approaches have limited domains of applicability, and can only be used either in the regime of strong (the BDMPS formalism [2, 5]) or weak (the GLV formalism [6]) LPM suppression (the GLV approach [6], in addition, is restricted to the emission of soft gluons). For this reason they can not be used for an accurate analysis of jet quenching for RHIC (and LHC) conditions.

The LCPI approach expresses the gluon spectrum through a solution of a two-dimensional Schrödinger equation with an imaginary potential in the impact parameter plane. The imaginary potential is proportional to the cross section of interaction of the $\bar{q}qg$ system (for $q \to gq$ transition) with a particle in the medium, $\sigma_3(\rho)$ (here ρ is the transverse distance between quark and gluon, the antiquark is located at the center of mass of the qg-system). The $\sigma_3(\rho)$ can be written as $\sigma_3(\rho) = C(\rho)\rho^2$. The factor $C(\rho)$ has a smooth (logarithmic) dependence on ρ for $\rho \ll 1/\mu_D$ (hereafter μ_D is the Debye screening mass). If one replaces $C(\rho)$ by $C(\rho_{\text{eff}})$, where ρ_{eff} is the typical value of ρ, the Hamiltonian takes the oscillator form. This approximation, simplifying greatly the calculations, was employed in several analyses [4, 7, 13] (it was also used in the BDMPS approach [2, 5]). However, the oscillator approximation turns out to be too crude and unsatisfactory. First of all for RHIC and LHC conditions the dominating ρ scale is not small enough and the results depend strongly on the choice of ρ_{eff}. Another reason why the oscillator approximation is unsatisfactory is more serious. In the high energy limit the gluon formation length, L_f, becomes larger than the quark pathlength in the QGP, and finite-size effects become important. In this regime $\rho_{\text{eff}} \ll 1/\mu_D$, and one might have expected naively that the oscillator approximation should work very well. However, one can show [14] that in this regime the dominating $N = 1$ rescattering contribution (and any odd rescattering) evaluated in the oscillator approximation simply vanishes. For RHIC and LHC conditions the finite-size effects play a very important role, and the oscillator approximation can lead to uncontrolled errors. For this reason one has to use an accurate parametrization of the three-body cross section. It requires numerical calculations for solving the Schrödinger equation.

In the present paper we represent the induced gluon spectrum in a new form which is convenient for numerical computations. We, for the first time, calculate the induced gluon emission and the nuclear modification factor for RHIC conditions using a realistic imaginary potential.

2. We consider a quark with energy E produced in a medium at $z = 0$ (we chose the z-axis along the quark

[1)]Supported by DFG-grant Schi 189/6-1

momentum). The induced gluon spectrum in the gluon fractional longitudinal momentum x reads [3]

$$\frac{dP}{dx} = 2\mathrm{Re}\int_0^\infty dz_1 \int_{z_1}^\infty dz_2 g(x)\,[K(z_2,\boldsymbol{\rho}_2|z_1,\boldsymbol{\rho}_1) - \\ - K_v(z_2,\boldsymbol{\rho}_2|z_1,\boldsymbol{\rho}_1)]\Big|_{\boldsymbol{\rho}_1=\boldsymbol{\rho}_2=0}. \quad (1)$$

Here K is the Green's function for the Hamiltonian (acting in the transverse plane)

$$H = -\frac{1}{2M(x)}\left(\frac{\partial}{\partial\boldsymbol{\rho}}\right)^2 + v(\boldsymbol{\rho},z) + \frac{1}{L_f}, \quad (2)$$

$$v(\boldsymbol{\rho},z) = -i\frac{n(z)\sigma_3(\rho)}{2}, \quad (3)$$

and

$$K_v(z_2,\boldsymbol{\rho}_2|z_1,\boldsymbol{\rho}_1) = \\ = \frac{M(x)}{2\pi i(z_2-z_1)}\exp\left[\frac{iM(x)(\boldsymbol{\rho}_2-\boldsymbol{\rho}_1)^2}{2(z_2-z_1)} - \frac{i(z_2-z_1)}{L_f}\right] \quad (4)$$

is the Green's function for the Hamiltonian (2) with $v(\boldsymbol{\rho},z) = 0$. In (2) the Schrödinger mass is $M(x) = Ex(1-x)$, $L_f = 2Ex(1-x)/[m_q^2x^2 + m_g^2(1-x)]$ is the gluon formation length, here m_q and m_g are the quark and gluon masses which play the role of the infrared cutoffs at $x \sim 1$ and $x \sim 0$ (in the QGP $m_{q,g}$ are given by the quark and gluon quasiparticle masses). In (3) $n(z)$ is the number density of QGP, and σ_3 is the above mentioned cross section of the color singlet $q\bar{q}g$ system with a particle in the medium. Summation over triplet (quark) and octet (gluon) color states is implicit in (3). The σ_3 may depend on z (through the Debye screening mass), however, below we will use z-independent μ_D. The vertex factor $g(x)$, entering (1), reads

$$g(x) = \frac{\alpha_s P(x)}{2M^2(x)}\frac{\partial}{\partial\boldsymbol{\rho}_1}\cdot\frac{\partial}{\partial\boldsymbol{\rho}_2}, \quad (5)$$

where $P(x) = C_F[1+(1-x)^2]/x$ is the splitting function for the $q \to gq$ transition (C_F is the quark Casimir factor). Note that we neglect the spin-flip $q \to qg$ transition, which gives a small contribution to the quark energy loss.

The three-body cross section entering the potential (3) can be written as [15, 3]

$$\sigma_3(\rho) = \frac{9}{8}[\sigma_{q\bar{q}}(\rho) + \sigma_{q\bar{q}}((1-x)\rho)] - \frac{1}{8}\sigma_{q\bar{q}}(x\rho), \quad (6)$$

where

$$\sigma_{q\bar{q}}(\rho) = \alpha_s^2 C_T C_F \int d\mathbf{q}\frac{[1-\exp(i\mathbf{q}\boldsymbol{\rho})]}{(q^2+\mu_D^2)^2} \quad (7)$$

is the dipole cross section for the color singlet $q\bar{q}$ pair (C_T is the color Casimir for the thermal parton (quark or gluon)).

The spectrum (1) can be rewritten as (L is the quark pathlength in the medium)

$$\frac{dP}{dx} = \int_0^L dz\, n(z)\frac{d\sigma_{\mathrm{eff}}^{BH}(x,z)}{dx}, \quad (8)$$

$$\frac{d\sigma_{\mathrm{eff}}^{BH}(x,z)}{dx} = \mathrm{Re}\int_0^z dz_1 \int_z^\infty dz_2 \times \\ \int d\boldsymbol{\rho}\, g(x) K_v(z_2,\boldsymbol{\rho}_2|z,\boldsymbol{\rho})\sigma_3(\rho)K(z,\boldsymbol{\rho}|z_1,\boldsymbol{\rho}_1)\Big|_{\boldsymbol{\rho}_1=\boldsymbol{\rho}_2=0}. \quad (9)$$

The $d\sigma_{\mathrm{eff}}^{BH}/dx$ (9) can be viewed as an effective Bethe–Heitler cross section which accounts for the LPM and finite-size effects. One can represent (9) as

$$\frac{d\sigma_{\mathrm{eff}}^{BH}(x,z)}{dx} = -\frac{\alpha_s P(x)}{\pi M(x)}\mathrm{Im}\int_0^z d\xi\,\frac{\partial}{\partial\rho}\left(\frac{F(\xi,\rho)}{\sqrt{\rho}}\right)\Big|_{\rho=0}, \quad (10)$$

where the function F is the solution of the radial Schrödinger equation for the azimuthal quantum number $m = 1$

$$i\frac{\partial F(\xi,\rho)}{\partial\xi} = \left[-\frac{1}{2M(x)}\left(\frac{\partial}{\partial\rho}\right)^2 - i\frac{n(z-\xi)\sigma_3(\rho)}{2} + \\ + \frac{4m^2-1}{8M(x)\rho^2} + \frac{1}{L_f}\right]F(\xi,\rho). \quad (11)$$

The boundary condition for $F(\xi,\rho)$ reads $F(\xi=0,\rho) = \sqrt{\rho}\sigma_3(\rho)\epsilon K_1(\epsilon\rho)$, where $\epsilon = [m_q^2x^2 + m_g^2(1-x)^2]^{1/2}$, and K_1 is the Bessel function. In deriving (10) we have used the relations [9]

$$\frac{\partial}{\partial\boldsymbol{\rho}_1}\cdot\frac{\partial}{\partial\boldsymbol{\rho}_2} = \frac{1}{2}\left[\left(\frac{\partial}{\partial x_1} - i\frac{\partial}{\partial y_1}\right)\cdot\left(\frac{\partial}{\partial x_2} + i\frac{\partial}{\partial y_2}\right) + \\ + \left(\frac{\partial}{\partial x_1} + i\frac{\partial}{\partial y_1}\right)\cdot\left(\frac{\partial}{\partial x_2} - i\frac{\partial}{\partial y_2}\right)\right],$$

$$\left(\frac{\partial}{\partial x_2} \pm i\frac{\partial}{\partial y_2}\right)\int_z^\infty dz_2 K_v(z_2,\boldsymbol{\rho}_2|z,\boldsymbol{\rho}) = \\ = \pm\frac{M(x)}{i\pi}\exp(\pm i\phi)K_1(\epsilon\rho).$$

The time variable ξ in (10) in terms of the variables z and z_1 of Eq. (9) is given by $\xi = z - z_1$, i.e., contrary to the Schrödinger equation for the Green's functions entering (1), (10) represents the spectrum through the solution to the Schrödinger equation which describes evolution of the $q\bar{q}g$ system back in time. It allows one to have a smooth boundary condition which is convenient for numerical calculations.

3. The jet quenching is usually characterized by the nuclear modification factor (we consider the central rapidity region $y \sim 0$ and suppress the explicit y-dependence)

$$R_{AA}(p_T) = \frac{d\sigma^{AA}(p_T)/dydp_T^2}{N_{bin}d\sigma^{pp}(p_T)/dydp_T^2}, \qquad (12)$$

where $d\sigma^{AA}/dydp_T^2$ and $d\sigma^{pp}/dydp_T^2$ are the inclusive cross section for $A+A$ and $p+p$ collisions, N_{bin} is the number of the binary nucleon-nucleon collisions. The effect of parton energy loss on the high-p_T hadron production in $A+A$ collisions can approximately be described in terms of effective hard partonic cross sections which account for the induced gluon emission [16]. Using the power-low parametrization for cross section of quark production in $p+p$ collisions $\propto 1/p_T^{n(p_T)}$ one can obtain

$$R_{AA}(p_T) \approx P_0(p_T) + \\ + \frac{1}{J(p_T)} \int_0^1 dz z^{n(p_T)-2} D_q^h(z, \frac{p_T}{z}) \times \\ \times \int_0^1 dx (1-x)^{n(p_T/z)-2} \frac{dI\left(x, \frac{p_T}{z(1-x)}\right)}{dx}, \qquad (13)$$

$$J(p_T) = \int_0^1 dz z^{n(p_T)-2} D_q^h(z, \frac{p_T}{z}), \qquad (14)$$

where P_0 is the probability of quark propagation without induced gluon emission, $dI(x,p_T)/dx$ is the probability distribution in the quark energy loss for a quark with $E = p_T$, $D_q^h(z, p_T/z)$ is the quark fragmentation function. Note that since $n(p_T) \gg 1$ the z-integrands in (13), (14) are sharply peaked at $z \approx \bar{z}$ ($\bar{z}$ is the value of z at which $z^{n(p_T)-2}D_q^h(z,p_T/z)$ has a maximum). For this reason (13) to a quite good accuracy can be approximated as

$$R_{AA}(p_T) \approx P_0(p_T) + \\ + \int_0^1 dx (1-x)^{n(p_T/\bar{z})-2} \frac{dI\left(x, \frac{p_T}{\bar{z}(1-x)}\right)}{dx}. \qquad (15)$$

We take the P_0 and spectrum in the radiated energy entering (13) in the form

$$P_0(E) = \exp\left(-\int_{x_{\min}}^1 dx \frac{dP(x,E)}{dx}\right), \qquad (16)$$

$$\frac{dI(x,E)}{dx} = \frac{dP(x,E)}{dx} \cdot \exp\left(-\int_x^1 dy \frac{dP(y,E)}{dy}\right), \qquad (17)$$

where $x_{\min} \approx m_g/E$, and it is assumed that the spectrum equals zero at $x \le x_{\min}$. Formula (17) corresponds to the leading order term of the series in $L/L_{\rm rad}$ (here $L_{\rm rad}$ is the radiation length corresponding to the energy loss $\Delta E \sim E$) of the spectrum derived in [17] for the photon emission, and strictly speaking is only valid for $\Delta E \ll E$. However, even for more broad domain $\Delta E \lesssim E$ (which is interesting from the point of view of jet quenching at RHIC) (17) reproduces the energy loss spectrum evaluated assuming independent gluon radiation to a reasonable accuracy. An accurate calculation of the nuclear modification factor accounting for the higher order terms in $L/L_{\rm rad}$ in the approximation of independent gluon emission [16] does not make sense because this approximation itself does not have any theoretical justification. Note that our spectrum is automatically normalized to unity.

The effective exponent $n(p_T)$ for quark production entering (13) is close to that for hadron production, $n_h(p_T)$. A small difference between these quantities (stemming from the p_T dependence of the integral (14)) is given by $n(p_T) - n_h(p_T) = d\ln J(p_T)/d\ln p_T$. For Au+Au collisions at $\sqrt{s} = 200\,\mathrm{GeV}$ we use $n_h(p_T) = np_T/(p_T+b)$ with $n = 9.99$ and $b = 1.219$ corresponding to the parametrization $d\sigma/dydp_T^2 = A/(p_T+b)^n$ obtained in [18] for π^0 production in $p+p$ collisions. The above procedure allows one to avoid uncertainties of the pQCD calculations of the partonic cross sections.

4. To fix the $m_{q,g}$ and μ_D we use the results of the analysis of the lattice calculations within the quasiparticle model [19]. For the relevant range of temperature of the plasma $T \sim (1-3)T_c$ ($T_c \approx 170\,\mathrm{MeV}$ is the temperature of the deconfinement phase transition) the analysis [19] gives for the quark and gluon quasiparticle masses $m_q \approx 0.3$ and $m_g \approx 0.4\,\mathrm{GeV}$. With the above value of m_g from the perturbative relation $\mu_D = \sqrt{2}m_g$ one obtains $\mu_D \approx 0.57\,\mathrm{GeV}$. To study the infrared sensitivity of our results we also perform computations for $m_g = 0.75\,\mathrm{GeV}$ (with $\mu_D = 0.57\,\mathrm{GeV}$). This value of the infrared cutoff for gluon emission in parton-nucleon interaction has been obtained from the analysis of the low-x proton structure function within the dipole BFKL equation [15, 20]. It seems to be reasonable for gluon emission in the developed mixed phase and for fast gluons with $L_f \gtrsim L$. This value agrees well with the natural infrared cutoff for gluon emission in the vacuum $m_g \sim 1/R_c$, where $R_c \approx 0.27$ fm is the gluon correlation radius in the QCD vacuum [21]. The above two values of m_g give reasonable lower and upper limits of the infrared cutoff for the induced gluon emission for RHIC and LHC conditions.

We perform numerical calculations for fixed and running α_s. In the first case we take $\alpha_s = 0.5$ for gluon emission from light quarks and gluons, and $\alpha_s = 0.4$ for the case of c-quark. For the running α_s we use the parametrization (with $\Lambda_{QCD} = 0.3$ GeV) frozen at $\alpha_s = 0.7$ at low momenta. This parametrization is consistent with the integral of $\alpha_s(Q)$ in the interval $0 < Q < 2$ GeV obtained from the analysis of the heavy quark energy loss (in vacuum) [22]. Previously this parametrization has been used to describe successfully the HERA data on the low-x proton structure function within the dipole BFKL approach [15, 20]. To incorporate the running α_s in our formalism we include α_s in the integrand on the right-hand side of (10), and take for virtuality $Q^2 = aM(x)/\xi$. The parameter a was adjusted to reproduce the $N = 1$ rescattering contribution evaluated in the ordinary diagrammatic approach [23]. It gives $a \approx 1.85$. For the dipole cross section (7) we take $Q^2 = \mathbf{q}^2$.

We assume the Bjorken [24] longitudinal expansion of the QGP with $T^3\tau = T_0^3\tau_0$ which gives $n(z) \propto 1/z$ for $z > \tau_0$. We use the initial conditions suggested in [25]: $T_0 = 446$ MeV and $\tau_0 = 0.147$ fm for RHIC, and $T_0 = 897$ MeV and $\tau_0 = 0.073$ fm for LHC. For RHIC the above condition were obtained from the charged particle pseudorapidity density $dN/dy \approx 1260$ measured by the PHOBOS experiment [26] in Au+Au collisions at $\sqrt{s} = 200$ GeV assuming an isentropic expansion and rapid thermolization at $\tau_0 \sim 1/3T_0$. The LHC parameters correspond to $dN/dy \approx 5625$ at $\sqrt{s} = 5.5$ TeV estimated in [27]. The above initial conditions for RHIC (translated into $\tau_0 = 0.6$ fm) agrees with that used in successful hydrodynamic description of Au+Au collisions at RHIC [28]. Note that, since the dominating ρ-scale in (9) $\propto \sqrt{z}$ for $z \ll L_f$, our results are not very sensitive to τ_0 (for a given entropy). The maximum parton pathlength in the hot QCD medium is restricted by the life-time of the QGP (and mixed) phase[2)], $\tau_{\max}$. We take $\tau_{\max} \sim R_A \sim 6$ fm. This seems to be a reasonable value for central heavy-ion collisions since due to the transverse expansion the hot QCD matter should cool quickly at $\tau \gtrsim R_A$ [24].

In Fig.1 we show the induced gluon spectrum for $q \to gq$ transition for RHIC conditions for the quark

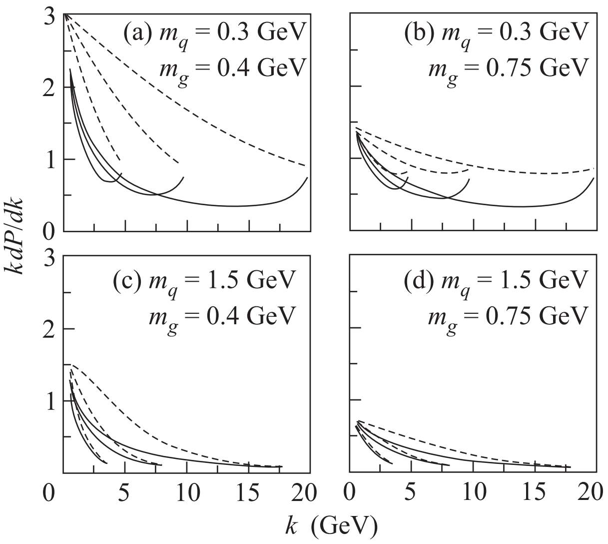

Fig.1. The induced gluon spectrum (solid line) for $q \to gq$ transition versus the gluon momentum k for RHIC conditions for $E = 5$, 10 and 20 GeV, $L = 6$ fm obtained using (8), (10) with $\alpha_s = 0.5$ for $m_q = 0.3$ GeV (a,b) and $m_q = 1.5$ GeV (c,d), $m_g = 0.4$ GeV (left) and 0.75 GeV (right). The Bethe-Heitler spectrum is shown by the dashed line

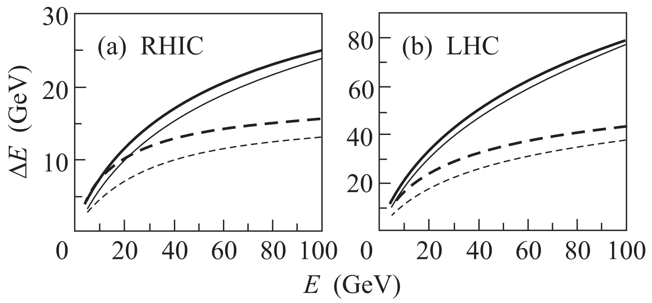

Fig.2. The energy dependence of the quark energy loss for RHIC (a) and LHC (b) for $L = 6$ fm obtained with $\alpha_s = 0.5$ (solid line) and running α_s (dashed line), $m_g = 0.4$ GeV (thick lines) and $m_g = 0.75$ GeV (thin lines), $m_q = 0.3$ GeV

pathlength $L = 6$ fm obtained with $m_q = 0.3$ and $m_q = 1.5$ GeV for $m_g = 0.4$ and $m_g = 0.75$ GeV. In Fig.1 we also show the Bethe-Heitler spectrum (dashed line). One sees that the LPM and finite-size effects suppress strongly the gluon emission. The gluon emission from c-quark is suppressed in comparison with light quark due to larger mass which leads to decreas-

[2)]For our choice of the initial conditions the life-time of QGP is ~ 3 fm for RHIC. However, in the interval $\tau \sim 3-6$ fm the density of the mixed phase is practically the same as that for the pure QGP phase.

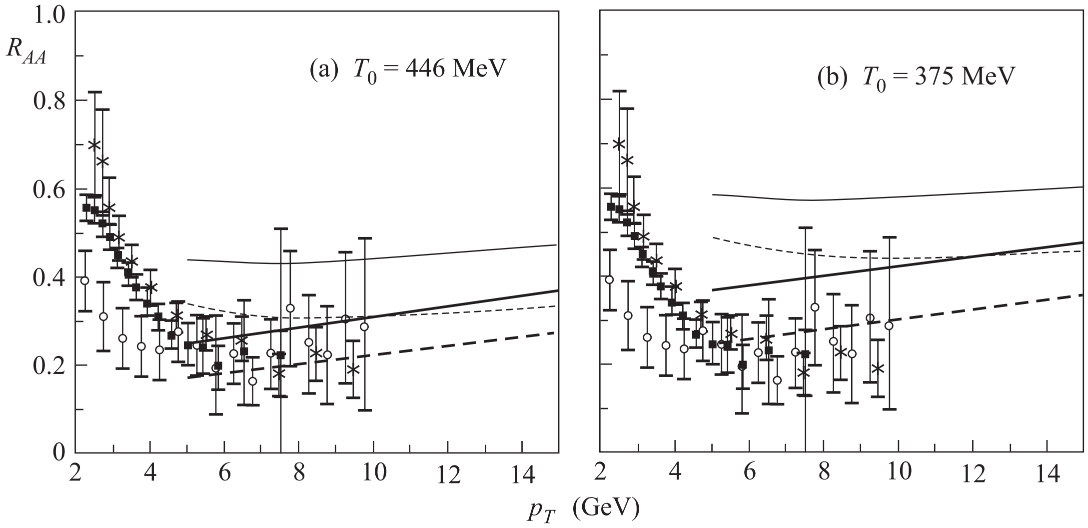

Fig.3. The nuclear modification factor (13) for central Au+Au collisions at $\sqrt{s} = 200$ GeV for quark (solid line) and gluon (dashed line) jets obtained with $m_g = 0.4$ GeV (thin lines) and $m_g = 0.75$ GeV (thick lines) for running α_s. The experimental points (from [1]) are for: circle – Au+Au→ $\pi^0 + X$ (0–10% central) [PHENIX Collaboration], square – Au+Au→ $h^\pm + X$ (0–10% central) [PHENIX Collaboration], star – Au+Au→ $h^\pm + X$ (0–5% central) [STAR Collaboration]

ing of the dominating ρ scale (note that the spectrum is not sensitive to the light quark mass, except for $x \sim 1$). One can see from Fig.1 that although the Bethe-Heitler spectrum differs strongly for two values of m_g, the difference becomes relatively small for the spectrum which accounts for the LPM and finite-size effects. It is connected with the fact that due to the multiple scattering and finite-size effects the dominating $1/\rho$-scale becomes larger than m_g, and namely this in-medium scale plays the role of the infrared cutoff at high energies [4] (however, of course, for not very high p_T the value of m_g is still important). We do not show the spectra for running α_s. They are similar in form (but somewhat suppressed at moderate fractional momenta). The LPM suppression for LHC is considerably stronger than for RHIC, but the spectra are similar in form and we do not show them as well.

In Fig.2 we plot the quark energy loss $\Delta E = E\int_{x_{\min}}^{1} dx x dP/dx$ evaluated for fixed (solid line) and running (dashed line) α_s for RHIC and LHC conditions for $L = 6$ fm with $m_g = 0.4$ GeV (thick lines) and $m_g = 0.75$ GeV (thin lines). The results for $\alpha_s = 0.5$ agree roughly with that for running α_s for $E \lesssim 10$ GeV but at higher energies the energy dependence is steeper for fixed α_s. It says that the typical ρ-scale becomes smaller with increasing energy. It is also seen from the decrease of the relative difference between the curves for $m_g = 0.4$ and 0.75 GeV.

In Fig.3a we compare the nuclear modification factor (13) for $T_0 = 446$ MeV calculated using the NLO KKP fragmentation functions [29] for running α_s with that obtained at RHIC [1] for central Au+Au collisions at $\sqrt{s} = 200$ GeV. For illustration of the dependence on T_0 in Fig.3b we present also the results for $T_0 = 375$ MeV. The theoretical curves have been obtained for $L = 4.9$ fm. It is the typical parton path-length in the QGP (and mixed) phase for $\tau_{max} = 6$ fm. We present the results for $m_g = 0.4$ and 0.75 GeV. For $p_T \lesssim 15$ the results for $\alpha_s = 0.5$ are close to that for running α_s and we do not plot them. The results for the quark (solid line) and gluon (dashed line) jets are shown separately (note that for $\sqrt{s} = 200$ GeV the quark and gluon contributions are compatible). The suppression is somewhat stronger for gluon jets. One can see from Fig.3a that the theoretical R_{AA} for $m_g = 0.4$ is in a reasonable agreement with the experimental one. One should bear in mind, however, that our calculations neglect the collisional energy loss [30]. For $p_T \sim 5-15$ GeV the collisional energy loss may increase the total energy loss by $\sim 30-40\%$. In this case (if one takes the initial conditions [25]) the value $m_g = 0.75$ GeV would be more preferable for agreement with the RHIC data. As mentioned previously, this value is reasonable for the mixed phase and for gluons with $L_f \gtrsim L$. Since for $\sqrt{s} = 200$ GeV the medium spends about half of its time in the mixed phase the effective infrared cutoff may be larger than the gluon quasiparticle mass in the QGP. For this reason the collisional energy loss may be included without using unrealistic infrared cutoff for the induced energy loss. Possible remaining small disagreement with the data may be avoided taking somewhat smaller value of T_0 (or α_s). In any case it is clear that for such a complicated phenomenon it is hardly possible to expect a perfect agreement with experiment, and the agreement found in the present paper is surprisingly good.

The above estimate for the collisional energy loss has been obtained for the pQCD plasma. Presently there are some indications [31] that the medium produced at RHIC may be a strongly coupled QGP. The radiative energy loss should not be very sensitive to the dynamics of the QGP (for the same number density of the QGP). However, it may be important for the collisional energy loss. Unfortunately, the corresponding calculations have not been made yet. It is interesting that our results give support for the scenario with strongly coupled QGP. Indeed, this scenario requires $\alpha_s \gtrsim 0.5$ [31] for thermal partons. The R_{AA} is sensitive to the radiation of soft gluons with the energy about a few μ_D. One can expect that for such gluons α_s should be close to that for thermal partons. We obtained agreement with the data with α_s which is frozen at the value 0.7 at low momenta. If α_s is frozen at a value below 0.4–0.5 the theoretical R_{AA} strongly disagrees with that observed at RHIC.

5. In summary, we have represented within the LCPI approach [3] the induced gluon spectrum in a new form convenient for numerical calculations, and carried out computations of the induced gluon emission from fast partons in the expanding QGP for RHIC and LHC conditions. The calculations for the first time have been performed with a realistic parametrization of the dipole cross section. The theoretical nuclear modification factor calculated for the initial conditions obtained from the charged particle rapidity density observed at RHIC [25] and hydrodynamic simulation of the RHIC data [28] is in a reasonable agreement with that observed at RHIC.

I thank R. Baier and D. Schildknecht for discussions and the kind hospitality at the University of Bielefeld, where this work was completed. I am also grateful to the High Energy Group of the ICTP for the kind hospitality during my visit to Trieste where a part of this work was done.

1. D. d'Enterria, *Invited overview talk at 39th Rencontres de Moriond on QCD and High-Energy Hadronic Interactions*, La Thuile, Italy, 28 Mar – 4 Apr 2004; nucl-ex/0406012.
2. R. Baier, Y. L. Dokshitzer, A. H. Mueller et al., Nucl. Phys. **B483**, 291 (1997); *ibid.* **B484**, 265 (1997).
3. B. G. Zakharov, JETP Lett. **63**, 952 (1996).
4. B. G. Zakharov, JETP Lett. **65**, 615 (1997).
5. R. Baier, Y. L. Dokshitzer, A. H. Mueller, and D. Schiff, Nucl. Phys. **B531**, 403 (1998).
6. M. Gyulassy, P. Lévai, and I. Vitev, Nucl. Phys. **B594**, 371 (2001).
7. U. A. Wiedemann, Nucl. Phys. **A690**, 731 (2001).
8. R. Baier, D. Schiff, and B. G. Zakharov, Ann. Rev. Nucl. Part. **50**, 37 (2000).
9. B. G. Zakharov, Phys. Atom. Nucl. **61**, 838 (1998).
10. B. G. Zakharov, JETP Lett. **70**, 176 (1999).
11. L. D. Landau and I. Ya. Pomeranchuk, Dokl. Akad. Nauk SSSR **92**, 535, 735 (1953).
12. A. B. Migdal, Phys. Rev. **103**, 1811 (1956).
13. C. A. Salgado and U. A. Wiedemann, Phys. Rev. Lett. **89**, 092303 (2002); C. A. Salgado and U. A. Wiedemann, Phys. Rev. **D68**, 014008 (2003).
14. B. G. Zakharov, JETP Lett. **73**, 49 (2001).
15. N. N. Nikolaev, B. G. Zakharov, and V. R. Zoller, Phys. Lett. **B328**, 486 (1994).
16. R. Baier, Yu. L. Dokshitzer, A. H. Mueller, and D. Schiff, JHEP **0109**, 033 (2001); hep-ph/0106347 (2001).
17. B. G. Zakharov, Phys. Atom. Nucl. **62**, 1008 (1999); JETP Lett. **78**, 759 (2003).
18. S. S. Adler et al., [PHENIX Collaboration], Phys. Rev. Lett. **91**, 241803 (2003).
19. P. Lévai and U. Heinz, Phys. Rev. **C57**, 1879 (1998).
20. N. N. Nikolaev and B. G. Zakharov, Phys. Lett. **B327**, 149 (1994).
21. E. V. Shuryak, Rev. Mod. Phys. **65**, 1 (1993).
22. Yu. L. Dokshitzer, V. A. Khoze, and S. I. Troyan, Phys. Rev. **D53**, 89 (1996).
23. B. G. Zakharov, JETP Lett. **80**, 67 (2004).
24. J. D. Bjorken, Phys. Rev. **D27**, 140 (1983).
25. R. J. Fries, B. Müller, and D. K. Srivastava, Phys. Rev. Lett. **90**, 132301 (2003).
26. B. B. Back et al. [PHOBOS Collaboration], Phys. Rev. **C65**, 061901 (2002).
27. J. Kapusta, L. D. McLerran, and D. K. Srivastava, Phys. Lett. **B283**, 145 (1992).
28. U. W. Heinz and P. F. Kolb, Nucl. Phys. **A702**, 269 (2002).
29. B. A. Kniehl, G. Kramer, and B. Potter, Nucl. Phys. **B582**, 514 (2000).
30. J. D. Bjorken, Fermilab preprint Pub-82/59-THY (1982).
31. E. V. Shuryak, hep-ph/0405066; E. V. Shuryak and I. Zahed, hep-ph/0403127.